Supplemental Methods

Role of the hydrophobic and charged residues in the 218 to 226 region of apoA-I in the biogenesis of HDL

Secretion of WT and mutant apoA-I forms. To assess the secretion of WT and mutant apoA-I forms, SW1783 human astrocytoma (HTB-13) cells were grown to 80% confluence in Leibovitz's L-15 medium containing 2% heat-inactivated horse serum in 6-well plates. The cells were then infected with adenoviruses expressing WT and mutant apoA-I forms at a multiplicity of infection of 10. Twenty-four hours post-infection, the cells were washed twice with PBS and incubated in serum-free medium for 2 h. Following an additional wash with PBS, fresh serum-free medium was added, and 24 h later was collected and analyzed by SDS-PAGE for detection of apoA-I secreted into the culture medium.

Plasma lipids and apoA-I levels, FPLC fractionation, and two-dimensional gel electrophoresis.The concentration of total cholesterol and triglycerides of plasma drawn four days post-infection was determined using the Total Cholesterol E, Free Cholesterol C and Phospholipids C reagents respectively (Wako Chemicals USA, Inc., Richmond, VA). Triglycerides were determined using the INFINITY triglycerides reagent (ThermoScientific, Waltham, MA), according to the manufacturer's instructions. Plasma apoA-I levels were determined by a turbidometric assay using AutoKit A-I (Wako Chemical USA, Inc., Richmond, VA) (1;2). For FPLC analysis of plasma, 17 μl plasma obtained from mice infected with adenovirus-expressing WT or mutant apoA-I forms were loaded onto a Sepharose 6 PC column (Amersham Biosciences, Piscataway, NJ) in a SMART micro FPLC system (Amersham Biosciences, Piscataway, NJ) and eluted with PBS. A total of 25 fractions of 50 μl volume each were collected for further analysis. The concentration of lipids in the FPLC fractions was determined as described above. The plasma HDL subpopulations were separated by two-dimensional electrophoresis. The proteins were then transferred to a nitrocellulose membrane and human apoA-I or mouse apoE were detected by

immunoblotting, using the goat polyclonal anti-human apoA-I antibody AB740 (Chemicon International, Billerica, MA) and the goat polyclonal anti-mouse apoE antibody (Santa Cruz Biotechnology) respectively (3).

Western blot for ABCA1, apoA-IV and apoE. For the western blots, liver lysates or plasma fractions, separated by density gradient ultracentrifugation, were run on SDS polyacrylamide gels then transferred to a nitrocellulose membrane (GE Healthcare). The gels used were 6% for the detection of ABCA1 and 12% for the detection of the other proteins. The blots were probed with goat polyclonal anti-mouse apoE antibody (Santa Cruz Biotechnology) or goat polyclonal anti-mouse apoA-IV antibody (Santa Cruz Biotechnology) or rabbit polyclonal anti-mouse ABCA1 (Novus Biologicals). The secondary antibodies for detection were conjugated with horseradish peroxidase. The blots were developed using ECL (GE Healthcare).

Fractionation of plasma by density gradient ultracentrifugation and electron microscopy (EM) analysis of the apoA-I containing fractions. For this analysis, 300 µl of plasma obtained from adenovirus-infected mice was diluted with saline to a total volume of 0.5 mL and fractionated by density gradient ultracentrifugation. Following ultracentrifugation, 0.5 mL fractions were collected and analyzed by SDS-PAGE as described (3). Fractions 6-7 obtained by the density ultracentrifugation, that float in the HDL region, were analyzed by electron microscopy using a Philips CM-120 electron microscope.

ApoA-I and ABCA1 mRNA quantification. Total hepatic RNA was isolated by the Trizol® method (Invitrogen, Carlsbad, CA) according to the manufacturer's instructions. RNA samples were adjusted to 0.1 µg/µl and cDNA was produced using the high capacity reverse transcriptase cDNA kit (Applied Biosystems, Foster City, CA). ApoA-I and ABCA1 mRNA was quantified using Applied Biosystems Gene Array TaqMan® primers for apoA-I cDNA (Applied Biosystems, Foster City, CA, Cat# Hs00985000_g1), mouse ABCA1 cDNA (Applied Biosystems, Foster City, CA, Cat# Mm00442646_m1) and 18s rRNA (Cat#

4319413E) and the TaqMan® Gene expression PCR Master Mix (Applied Biosystems, Foster City, CA, Cat# 4370048), using the Applied Biosystems 7300 Real-Time PCR System (4).

Protein extraction from mouse livers. Total hepatic protein was isolated using RIPA buffer (1xPBS, 0.5% sodium deoxycholate, 1%NP-40, 0.1% SDS). An aliquot of 450 ul of RIPA buffer was used to homogenize the liver for 20 seconds. The homogenate was freeze/thawed 2 times in liquid nitrogen and a 37^{o}C waterbath. Subsequently it was incubated in ice for 30 minutes and finally centrifuged in 5000 rpm (~1680 g) for 10 minutes. The total protein was determined with a DC protein assay kit (BioRad).

Preparation of apoA-I for physicochemical measurements. Before all analyses, lyophilized wild-type or mutant apoA-I forms were dissolved at a final concentration of 0.2mg/mL in 8M guanidine hydrochloride in DPBS. The protein samples were incubated for 1h at room temperature and then dialyzed extensively against DPBS pH 7.4. The samples were centrifuged at 12000g for 10 min to remove any precipitated protein. The supernatant solutions were quantitated by measuring their absorbance at 280nm. The proteins were kept at low concentrations (~0.1mg/mL) on ice to avoid aggregation. All analyses were performed on freshly refolded protein.

Circular dichroism measurements*:* A Jasco-715 spectropolarimeter connected to a Jasco PTC-348 WI Peltier temperature controller was used to record the far-UV CD spectra of the ApoA-I samples from 190 to 260nm at 25^{o}C using a quartz cuvette with an optical path of 1nm. The protein samples were at 0.1mg/mL in DPBS (pH 7.4). The measurement parameters were as follows: bandwidth 1nm, response 8sec, step size 0.2nm and scan speed 50nm/min. Each spectrum was the average of 5 accumulations. The results were corrected by subtracting the buffer baseline.

Helical content was calculated based on the molar ellipticity at 222nm as described by Greenfield et al. (5) using the equation: $\%\alpha\text{-helix}_{222nm}=([\Theta]_{222}+3000)/(36000+3000)\times100$.

To record the thermal denaturation profile of the protein, we monitored the change in molar ellipticity at 222nm, while the temperature was raised from 20 to 80˚C, at a rate of 1˚C/min. The curve was fitted to a Boltzman sigmoidal model curve using the Graphpad Prism™ software.

Chemical denaturation. To record the chemical denaturation profile of ApoA-I, 0.1 mg/mL of freshly refolded protein was added to a 4 mL quartz fluorimeter cuvette and the intrinsic tryptophan protein fluorescence was measured after excitation at 295 nm. Small amounts of an 8.0 M guanidine hydrochloride (Applichem) solution were gradually added in the cuvette. The contents were continuously mixed using a magnetic stirrer. After each addition of guanidine hydrochloride, the sample was incubated in the dark for 2 min before measuring the fluorescence signal.

8-anilino-1-naphthalene-sulfonate (ANS) fluorescence. 1,8 ANS (1-anilinonaphthalene-8-sulfonic acid, Sigma-Aldrich) was dissolved in dimethylsulfoxide (DMSO) to a final concentration of 50 mM (ANS stock solution). Freshly refolded ApoA-I at 0.05mg/ml in DPBS pH 7.4 was placed in a 4 mL quartz fluorimeter cuvette (Hellma, Germany). Fluorescence measurements were performed in a Quantamaster 4 fluorescence spectrometer (Photon Technology International, New Jersey). The scan rate was 1 nm/s with excitation at 395 nm and emission range from 420 to 550 nm. After measuring the background protein fluorescence, 7.5 μL of ANS stock solution were added in the cuvette and mixed so that the final ANS concentration was 250 μM. A control ANS spectrum in the absence of protein was also recorded.

Supplemental Table 1: Nucleotide sequence of primers used in PCR amplifications

Name	Sequence	Location of sequence
apoA-I [L218A/L219A/ V221A/L222A]F	5′- G GAC CTC CGC CAA GGC **GC**[a]G **GC**G CCC G**C**G **GC**G GAG AGC TTC AAG GTC **-3′**	nt 743-788[b] (sense) (aminoacids +212 to +227)[c]
apoA-I [L218A/L219A/ V221A/L222A]R	5′- GAC CTT GAA GCT CTC C**GC** C**G**C GGG C**GC** C**GC** GCC TTG GCG GAG GTC C **-3′**	nt 788-743 (antisense) (aminoacids +227 to +212)
apoA-I [E223A/K226A]R	5′- CTG CCC GTG CTG G**C**G AGC TTC **GC**G GTC AGC TTC CTG-3'	nt 762-797 (sense) (aminoacids +219 to +230)
apoA-I [E223A/K226A]R	5′- CAG GAA GCT GAC C**GC** GAA GCT C**G**C CAG CAC GGG CAG-3'	nt 797-762 (antisense) (aminoacids +230 to +219)
LCAT F	5′- GA ***AGA TCT***[d] ACC ATG GGG CCG CCC GGC TCC CCA- 3′	-
LCAT R	5′- GCG ***GAT ATC***[d] CTA TTC AGG AGG CGG GGG CTC TGG - 3′	-

[a]Mutagenized residues are marked in boldface type and are underlined.

[b]Nucleotide number of the human apoA-I cDNA sequence, oligonucleotide position is relative to the translation initiation ATG condon.

[c]Aminoacid position (+) refers to the mature plasma apoA-I sequence.

[d]The Bgl-II and EcoRV restriction sites.

Supplemental Table 2: Plasma lipids and hepatic mRNA levels of apoA-I$^{-/-}$ or apoA-I$^{-/-}$ x apoE$^{-/-}$ mice expressing wild type (WT) and the mutant forms of apoA-I as indicated.

Protein Expressed	Total Cholesterol *(mg/dL)*	Triglycerides *(mg/dL)*	Relative apoA-I mRNA (*%)*
WT apoA-I in apoA-I$^{-/-}$ mice	$^{(++)}$278 ± 74	78 ± 24	100 ± 26*
apoA-I [L218A/L219A/V221A/L222A] in apoA-I$^{-/-}$ mice	$^{(++)}$45 ± 14^{+}	50 ± 20	95 ±24
apoA-I [E223A/K226A] in apoA-I$^{-/-}$ mice	$^{(++)}$174 ± 53^{+}	115 ± 27^{+}	164 ± 82
WT apoA-I in apoA-I$^{-/-}$ x apoE$^{-/-}$ mice	1343 ± 104	294 ± 129	100 ± 13
apoA-I [L218A/L219A/V221A/L222A] in apoA-I$^{-/-}$ x apoE$^{-/-}$ mice	778 ± 52^{+}	18 ± 2^{+}	92 ± 23
apoA-I [L218A/L219A/V221A/L222A] plus LCAT in apoA-I$^{-/-}$ x apoE$^{-/-}$ mice	754 ± 122^{+}	37 ± 10^{+}	90 ± 3

($^{++}$) Cholesterol levels are those shown in figure 1.

Values are means ± standard deviation based on analysis of 5-6 mice per experiment. (*) Expression of apoA-I is relative to the expression of apoA-I WT in the apoA-I$^{-/-}$ or apoA-I$^{-/-}$ x apoE$^{-/-}$ mouse groups. Expression of LCAT was also confirmed by RT-PCR. Statistical significant differences in cholesterol and triglyceride levels at $p<0.05$ was calculated between mice expressing the WT apoA-I and the apoA-I[L218A/L219A/V221A/L222A] or apoA-I[E223A/K226A] mutant in either the apoA-I$^{-/-}$ or apoA-I$^{-/-}$ x apoE$^{-/-}$ mouse background and are indicated by a ($^{+}$).

Supplemental Figure 1

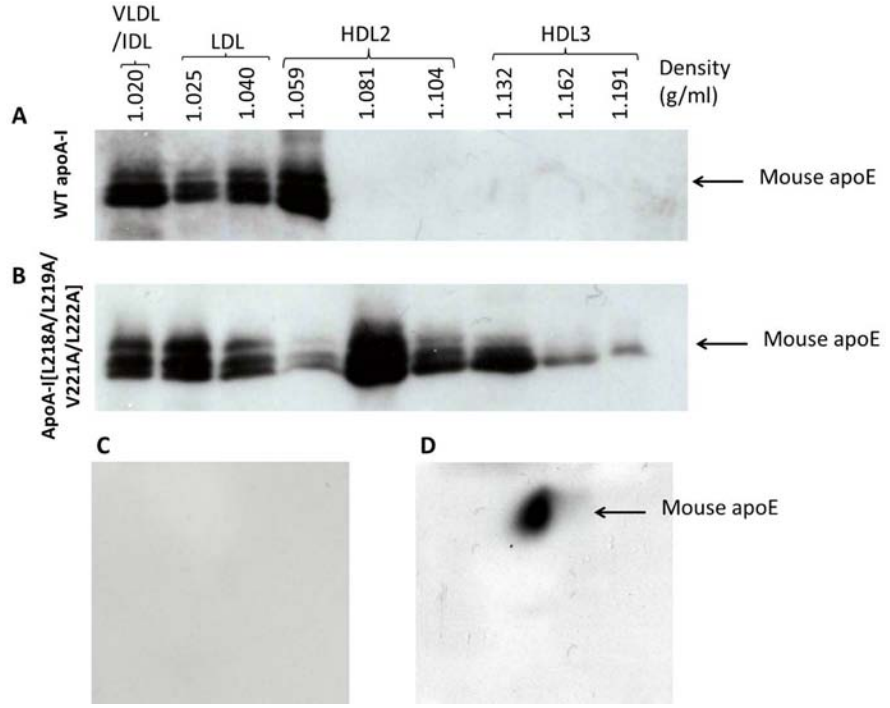

Supplemental Figure 1: Western blotting of plasma fractions obtained from apoA-I deficient mice expressing the WT apoA-I or the apoA-I[218-222] mutant following density gradient ultracentrifugation (A, B). The figure shows the absence of apoE in the HDL fractions of apoA-I deficient mice expressing the WT apoA-I (A) and strong presence of apoE in the HDL fractions of apoA-I deficient mice expressing the apoA-I[218-L222] mutant (B). Western blotting of the two dimensional gels of plasma obtained from apoA-I deficient mice expressing the WT apoA-I or the apoA-I[218-222] mutant with anti-mouse apoE antibody (C, D). The figure shows the absence of apoE-containing HDL in apoA-I deficient mice expressing the WT apoA-I (C) and the presence of apoE in apoA-I deficient mice expressing the apoA-I[218-222] mutant (D). The presence of mouse apoE in panels A-D was probed using a goat polyclonal anti-mouse apoE antibody.

Supplemental Figure 2:

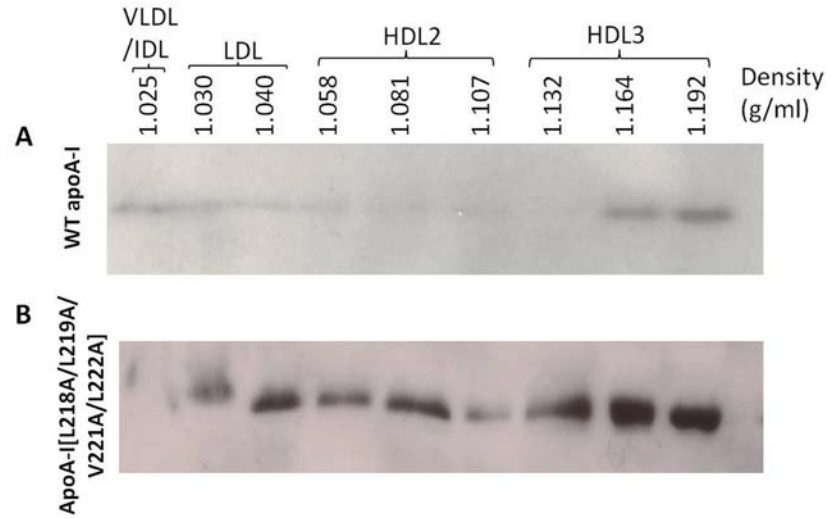

Supplemental Figure 2: Western blotting in apoA-I-/- x apoE-/- double deficient mice expressing the WT apoA-I or the apoA-I[218-222] mutant (A, B). The figure shows low levels of apoA-IV levels in mice expressing the WT apoA-I (A) and highly increased of apoA-IV in mice expressing the apoA-I[218-222] mutant (B). The presence of mouse apoA-IV in panels A, B was probed using an goat polyclonal anti-mouse apoA-IV antibody.

Supplemental Figure 3:

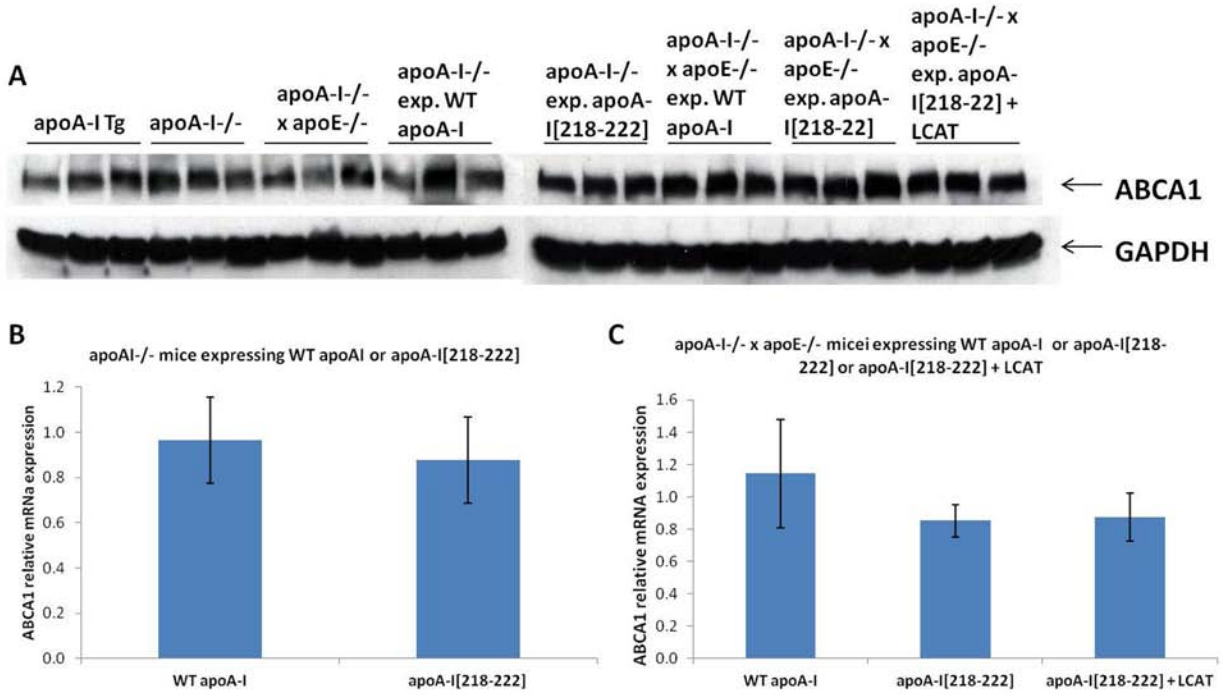

Supplemental Figure 3: Western blotting of hepatic extracts derived from apoA-I transgenic or apoA-I$^{-/-}$ or apoA-I$^{-/-}$ x apoE$^{-/-}$ double deficient mice without treatment or following adenovirus-mediated gene transfer of the WT apoA-I or the apoA-I[218-222] mutant (A). Hepatic ABCA1 mRNA levels derived from apoA-I$^{-/-}$ or apoA-I$^{-/-}$ x apoE$^{-/-}$ double deficient mice following adenovirus-mediated gene transfer of the WT apoA-I or the apoA-I[218-222] mutant (B, C). The differences in protein and mRNA levels between the groups were not statistically significant.

REFERENCES

1. Koukos, G., A. Chroni, A. Duka, D. Kardassis, and V. I. Zannis 2007. Naturally occurring and bioengineered apoA-I mutations that inhibit the conversion of discoidal to spherical HDL: the abnormal HDL phenotypes can be corrected by treatment with LCAT. *Biochem.J.* **406:** 167-174

2. Koukos, G., A. Chroni, A. Duka, D. Kardassis, and V. I. Zannis 2007. LCAT can rescue the abnormal phenotype produced by the natural ApoA-I mutations (Leu141Arg)Pisa and (Leu159Arg)FIN. *Biochemistry* **46:** 10713-10721

3. Chroni, A., H. Y. Kan, A. Shkodrani, T. Liu, and V. I. Zannis 2005. Deletions of helices 2 and 3 of human apoA-I are associated with severe dyslipidemia following adenovirus-mediated gene transfer in apoA-I-deficient mice. *Biochemistry* **44:** 4108-4117

4. Zhu, L. J. and S. W. Altmann 2005. mRNA and 18S-RNA coapplication-reverse transcription for quantitative gene expression analysis. *Anal.Biochem.* **345:** 102-109

5. Greenfield, N. and G. D. Fasman 1969. Computed circular dichroism spectra for the evaluation of protein conformation. *Biochemistry* **8:** 4108-4116